

Article

# New Insight into Electric Force in Metal and the Quadratic Electrical Resistivity Law of Metals at Low Temperatures

Vilius Palenskis 

Faculty of Physics, Vilnius University, Saulėtekio Av. 9, 10222 Vilnius, Lithuania; vilius.palenskis@ff.vu.lt

**Abstract:** Considering that Einstein's relation between the diffusion coefficient and the drift mobility of free randomly moving charge carriers in homogeneous materials including metals is always valid, it is shown that the effective electric force acting on free electrons in metal depends on the ratio between the kinetic free electron energy at the Fermi surface to the classical particle energy  $3kT/2$ . The electrical resistivity of elemental metals dependence on very low temperatures has the quadratic term, which has been explained by electron–electron scattering. In this paper, it is shown that the quadratic term of the electrical resistivity at low temperatures is caused by scattering of the free randomly moving electrons by electronic defects due to linear effective free electron scattering cross-section dependence on temperature, but not by electron–electron scattering.

**Keywords:** effective density of randomly moving (RM) electrons; density of states (DOSs); mean free electron path; effective electric force; electronic defects; effective scattering cross section; quadratic electrical resistivity law at low temperatures

## 1. Introduction

Investigation into electron transport in metals began over 100 years ago, when free electrons were postulated by Drude [1] to explain the conductivity of metals. At the same time, the properties of electrons in metals have been analyzed using classical statistical methods of the gases. It was assumed that the density of the free electrons is equal to the density of atoms and the mean free path of the electrons can be determined from comparison with experimentation. The Drude theory failed to explain why the electrons in a pure metal can freely travel over 100 atomic distances without being scattered. Later, it has been considered that all metal valence electrons become delocalized and are shared by all atoms in the solid, forming a “sea” of negative charge [2,3], and are no longer associated with a given atom [4]. The nuclei with their core electrons form ions, which are immersed in this sea of valence electrons. Such ungrounded theory about free electron transport in metals has continued for nearly the last century.

Usually, metal atoms are arranged in regular three-dimensional periodic lattices. Hard spheres of metal atoms are packed in such crystal structures: face-centered cubic (FCC), body-centered cubic (BCC), hexagonal close-packed (HCP), orthorhombic (ORC), and tetragonal (TET). The dependences of the metal atoms to various lattice structures and their distribution on the periodic table are presented in Figure 1 [5,6].

As can be seen from Figure 1, almost all metal atom packing density is close to the ideal close-packing value of 0.73, and it does not depend on the lattice structure. Only for Ga, Rb, Cs, and Sn is the packing density smaller than the ideal close-packing density value.

The interaction of the valence electrons with the ion cores produces the main contribution to the binding energy and lowering of the energy of the valence electrons in metal compared with the free atom, and this lowering causes the metallic binding [7–9]. The total number of bonds in metal is considerably large, and not all valence electron bonds have the same binding energy.



**Citation:** Palenskis, V. New Insight into Electric Force in Metal and the Quadratic Electrical Resistivity Law of Metals at Low Temperatures. *Metals* **2024**, *14*, 526. <https://doi.org/10.3390/met14050526>

Received: 14 March 2024

Revised: 27 April 2024

Accepted: 29 April 2024

Published: 30 April 2024



**Copyright:** © 2024 by the author. Licensee MDPI, Basel, Switzerland. This article is an open access article distributed under the terms and conditions of the Creative Commons Attribution (CC BY) license (<https://creativecommons.org/licenses/by/4.0/>).

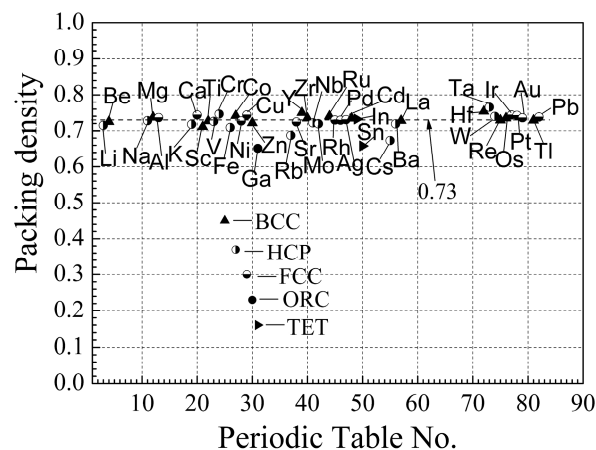


**Figure 1.** Packing density of various elemental metal distribution on the periodic table. Here, lattices: BCC—body-centered cubic; HCP—hexagonal close-packed; FCC—face-centered cubic; ORC—orthorhombic; TET—tetragonal. The dashed line (0.73) corresponds to the ideal close-packed lattice.

Some difficulties in the explanation of the electron transport in metals by classical statistics have been understood by quantum mechanics: the Pauli exclusion principle and Fermi-Dirac statistics. According to quantum mechanics, the free electrons as Bloch waves can freely move in the ideal periodic lattice of the metal without any scattering by lattice ions [3,7–10]. The scattering of the free electrons can be only in spots where there are distortions in periodicity of the potential energy of the ideal lattice structure.

The electrons in an ideal periodicity crystal are arranged in energy bands (allowed zones) separated by forbidden regions in energy (energy gaps). Each primitive cell exactly contributes only one independent value of the wave vector  $\mathbf{k}$  to each energy band [10–12]. The valence electrons occupy the lowest energy levels in the conduction band below the Fermi-level energy, and their distribution in energy  $E$  is described by the Fermi distribution function  $f(E)$ . Though the valence electron wave functions overlap with those of neighbor atoms [6–8], they remain associated with native ion cores. Only valence electrons, which have energies close to Fermi-level energy due to lattice atom vibrations, can be released, and can randomly move in metal [13,14]. The effective density  $n_{\text{eff}}$  of the free randomly moving (RM) electrons in metals and other materials has been defined in [15] as:

$$n_{\text{eff}} = \int_0^{\infty} g(E)f(E)[1 - f(E)]dE \quad (1)$$

where  $g(E)$  is the density of states (DOS) in the conduction band. It shows that the effective density  $n_{\text{eff}}$  of the free RM electrons in metals can be described as  $n_{\text{eff}} = g(E_F)kT$ , where  $g(E_F) = g(E)$  at  $E = E_F$ . It also lets us show that the Einstein relation between the diffusion coefficient  $D$  and the drift mobility  $\mu_{\text{drift}}$  of the free RM charge carriers  $D/\mu_{\text{drift}} = kT/q$  is valid in all cases with one type of charge carrier. In [16], for the first time, the probability density function of the free RM electron distribution on energy is presented:  $p(E) = f(E)[1 - f(E)]/kT$ , which meets all the requirements of the probability theory [17,18].

Though the value of the  $n_{\text{eff}}$  reaches only a small percentage of the total density  $n$  of the valence electrons of metals at room temperature, the total density of the valence electrons  $n$  has been traditionally used for the description of the electrical conductivity  $\sigma$  in metals and superconductors in the normal state by  $\sigma = q^2 n \tau / m^*$ , where  $q$ ,  $\tau$ , and  $m^*$  are the electron charge, the average electron relaxation time, and its effective mass, respectively. From a comparison of the Drude and Sommerfeld conductivity formulae, it has been stated that there is only a difference in the definition of the relaxation time of the free electrons [10]. The Drude conductivity formula can be used for descriptions of the conductivity of weakly

doped semiconductors, but it is completely inapplicable to describe the conductivity of metals and other materials with degenerate electron gas.

The resistivity of metal linear increase with a temperature above Debye's temperature was usually explained by charge carriers scattering due to lattice atom vibrations, due to an increase in the electron scattering cross section [6,9–12,19–22]. As shown in [13,14], the electron scattering cross section at a temperature above the Debye temperature does not depend on temperature, and the lattice vibrations play another role: they produce the free RM electrons, and at the same time they produce the electronic defects (weakly screened ions, which have lost valence electrons). The effective density of the electronic defects can be expressed as  $N_{\text{eff}} = n_{\text{eff}}$ . The remaining part  $N - N_{\text{eff}}$  of atoms that have valence electrons with energy lower than Fermi-level energy because thermal vibration energy is not sufficient to excite their valence electrons. As pointed out in [13], the remaining part  $n - n_{\text{eff}}$  of the valence electrons, whose energy is lower by a few  $kT$  than Fermi-level energy, due to the Pauli exclusion principle and Fermi-Dirac statistics, cannot change their energy, and they cannot scatter the free RM electrons.

In our earlier work [14–16], we presented results on the effective density of free randomly moving (RM) electrons and the effective density of electronic defects in elemental metals, the diffusion coefficient, and drift mobility of free RM electrons, as well as presenting an explanation of Hall effect peculiarities in elemental metals. In this work, there for the first time, a new insight into the electric force acting on free electrons in a metal and an explanation of the quadratic term of the electrical resistivity of elemental metals at very low temperatures is presented.

## 2. Effective Drift Velocity of Free RM Electrons and Effective Electric Force Acting on Free Electrons in Metals

The current density  $\mathbf{j}$  in homogeneous material is described as:

$$\mathbf{j}_x = \sigma \mathbf{E}_x = q n_{\text{eff}} \mathbf{v}_{x \text{ drift}} = q n_{\text{eff}} \mu_{\text{drift}} \mathbf{E}_x \quad (2)$$

where  $\sigma$  is the conductivity of the material,  $\mathbf{E}_x$  is the external applied electric field strength in the  $x$ -direction,  $n_{\text{eff}}$  is the effective density of the free randomly moving electron density,  $\mathbf{v}_{x \text{ drift}}$  is their drift velocity in the electric field, and  $\mu_{\text{drift}}$  is the free electron drift mobility.

Considering that Einstein's relation between the diffusion coefficient  $D$  and the drift mobility  $\mu_{\text{drift}}$  is valid for free RM electrons in metal, one can express the drift mobility of the free RM electrons in the following way:

$$\mu_{\text{drift}} = \frac{qD}{kT} = \frac{q \langle v^2 \rangle \langle \tau \rangle}{3kT} = \frac{q \langle \tau \rangle}{m^*} \cdot \frac{\langle E \rangle}{(3/2)kT} = \frac{q \langle \tau \rangle}{m^*} \cdot \alpha_\varepsilon \quad (3)$$

where the parameter  $\alpha_\varepsilon = \langle E \rangle / [(3/2) kT]$  shows how many times the average free RM electron kinetic energy exceeds the average classical particle energy  $(3/2) kT$ . Therefore, the drift velocity of the free RM electron can be described as:

$$\mathbf{v}_{x \text{ drift}} = \frac{\langle \tau \rangle}{m^*} \cdot \alpha_\varepsilon q \mathbf{E}_x = \frac{\langle \tau \rangle}{m^*} \mathbf{F}_{x\text{eff}} \quad (4)$$

where  $\mathbf{F}_{x\text{eff}}$  is the effective electric force acting on the free RM electron in the material. In the case of semiconductors with non-degenerate electron gas,  $\alpha_\varepsilon = 1$ , and:

$$\mathbf{F}_{x\text{eff}} = q \mathbf{E}_x \quad (5)$$

i.e., the effective electric force is described by the usual relation. Though the average drift velocity contribution to the direct current in materials without degenerate electron gas with and without accounting the electron distribution on energy gives the same result, the

electrons with higher velocities make a relatively higher contribution to the total current. In the case of metals, the effective electric force acting on the free RM electrons is equal to:

$$\mathbf{F}_{\text{xeff}} = \alpha_\varepsilon q \mathbf{E}_x = \frac{E_F}{(3/2)kT} q \mathbf{E}_x \quad (6)$$

The impulse of force  $\mathbf{I}$  acting on the free electrons during their scattering by electronic defects is:

$$\mathbf{I} = \mathbf{F}_{\text{eff}} \Delta t = \alpha_\varepsilon q \mathbf{E}_{\text{def}} \Delta t \quad (7)$$

where  $\Delta t$  is the acting time and  $\mathbf{E}_{\text{def}}$  is the electric field strength produced by the electronic defect. On the other hand,  $\mathbf{F}_{\text{eff}} = \Delta \mathbf{p} / \Delta t = \hbar \Delta \mathbf{k} / \Delta t$  (here,  $\mathbf{p}$  is the momentum and  $\mathbf{k}$  is the wave vector of the electron). If the average energy of the free electron during scattering change is about  $1.64 kT$  [14], the wave vector due to parameter  $\alpha_\varepsilon$  undergoes a very large change in direction.

Thus, the free electron motion in the material must be described by a general equation:

$$m \frac{d\mathbf{v}_{\text{drift}}}{dt} = q \alpha_\varepsilon \mathbf{E} - \frac{m \mathbf{v}_{\text{drift}}}{\langle \tau \rangle} \quad (8)$$

which is valid for homogeneous materials at any degree of degeneration of electron gas. In stationary state  $d\mathbf{v}_{\text{drift}}/dt = 0$ ,  $\mathbf{v}_{\text{drift}}$  is described by Equation (4).

Similarly, the free electron motion in electric and magnetic fields can be described as:

$$m \frac{d\mathbf{v}_{\text{drift}}}{dt} = q(\alpha_\varepsilon \mathbf{E} + \mathbf{v} \times \mathbf{B}) - \frac{m \mathbf{v}_{\text{drift}}}{\langle \tau \rangle} \quad (9)$$

where  $\mathbf{B}$  is the magnetic flux density. For static electric and magnetic fields, this equation can be presented as:

$$q(\alpha_\varepsilon \mathbf{E} + \mathbf{v} \times \mathbf{B}) = \frac{m \mathbf{v}_{\text{drift}}}{\langle \tau \rangle} \quad (10)$$

The solution of this equation for the Hall coefficient  $R_H$  gives the well-known result [14]:

$$R_H \sigma_0 = \frac{q \langle \tau \rangle}{m^*} r_H = \mu_H \quad (11)$$

where  $\sigma_0$  is the material conductivity at  $\mathbf{B} = 0$ ,  $r_H$  is the Hall factor and  $\mu_H$  is the Hall mobility. So, in the general case  $\mu_{\text{drift}} = \mu_H \alpha_\varepsilon / r_H$ , for the non-degenerate electron gas  $\mu_{\text{drift}} = \mu_H / r_H$ , and for metals and materials with highly degenerate electron gas  $\mu_{\text{drift}} = \mu_H \alpha_\varepsilon$ , can many times exceed the Hall mobility.

The fact that the free electron mean path is 100 times larger than the atomic distance, especially at low temperatures, where the mean free path is in the tens of millimeters, shows that the displacement of atoms from their equilibrium positions due to thermal vibrations weakly distorts the potential periodicity in the lattice. The free RM electrons are scattered only at electronic defects with absorption and emission of phonons. Usually, a single phonon takes place, because multiple-phonon process contribution is less probable. This is related to the fact that in thermal equilibrium conditions, the lattice atom vibration energy is small. On the other hand, the electron energy distribution is limited by the Pauli exclusion principle and Fermi–Dirac statistics. The statement that in a perfect crystal below the Debye temperature, the scattering angle becomes smaller and smaller and that it causes the resistivity  $T^5$ -law at low temperatures is ungrounded [13] because valence electrons whose energy is lower than  $E_F$  by at least several units of  $kT$  due to the Pauli exclusion principle and Fermi–Dirac statistics are not affected by lattice vibrations and the electron mean free path extends over hundreds of lattice constants. As it follows from Equation (7), the free electron wave vector during scattering at electronic defect change  $\Delta \mathbf{k}$  is very remarkable due to the multiplier  $\alpha_\varepsilon$ , and after each collision with the electronic defect, the free electron wave vector is completely randomized.

### 3. Study of the Electrical Resistivity Law $AT^2$ of Metals at Very Low Temperatures

The idea that electron–electron scattering contributes to the electrical and thermal resistivities of metals was proposed by Landau and Pomeranchuk [23], but for about 20 years, the resistivity dependence  $\rho_{ee}(T) = A_{ee}T^2$  has not been observed in simple metal. On the basis of the conservation of the quasi-momentum and energy of free electrons, it has been proposed that the electron–electron scattering rate changes as  $AT^2$ , and as a consequence, it must give the law  $AT^2$  of the electrical resistivity at very low temperatures. According to [9], the electron–electron scattering rate  $\tau_{ee}^{-1}(\varepsilon)$  can be described as:

$$\frac{1}{\tau_{ee}} = A_0 \frac{1}{\hbar} \frac{(kT)^2}{E_F} \quad (12)$$

where  $A_0$  is a non-dimensional quantity. Accounting this relation, it has been believed that relaxation time changes as  $1/T^2$ , and that this can take place only at very low temperatures in very pure metals. It also follows that temperature dependence of resistivity  $\rho(T)$  for a three-dimensional metal due to electron–electron scattering can be described as  $\rho(T) = AT^2$ .

A detailed analysis of electron–electron scattering and its contribution to the electrical resistivity for conducting materials is presented in [24]. The problem of electron–electron scattering in metals has also been solved using the Boltzmann kinetic equation [25]. Recently [26], it was shown that Equation (12) is correct with  $A_0 = N_{\text{imp}}/4\pi^2$ , where  $N_{\text{imp}}$  is the number of impurities (or scattering centers) in a given sample. The effects of electron–electron scattering in metals have also been investigated theoretically in both a simple tight-binding model and in the transition metal tungsten by calculating the electron scattering rate at the Fermi surface [27].

Considering that the contribution of the term  $AT^2$  to resistivity at very low temperatures is very small, and extremely precise measurement technique was needed, better than p.p.m. relative accuracy in the measurement of the low-temperature electrical resistivity, which appeared only a half-century ago [24,28–30]. High-resolution measurements of the electrical resistivity of simple metals at low temperatures yielded new data that were in contradiction to the generally accepted theories. It was found that electrical resistivity does not follow the expected  $AT^5$  law for any metal at very low temperatures.

A detailed analysis of the electrical resistivity of the alkali metals at low temperatures is presented in [24,31,32]. It is shown that for potassium at low temperatures, phonon drag can play an important role, leading to an exponential decrease with temperature [33,34]. It has been believed that the experimental parameter  $A_{\text{exp}}$  would be the same for all samples of the same metal, but the values  $A_{\text{exp}}$  are different by about 10-fold. For lithium, it was expected that values  $A_{\text{exp}}$  would be similar to K, but the observed values are more than an order larger [24,35,36].

The electrical resistivity of noble metals at low temperatures has been investigated by many authors [37–40]. It has been shown that the electrical resistivity of copper and silver at low temperatures has approximate  $T^4$  behavior, and the term  $T^2$  appears only below 2 K [37]. From the measurement of the electrical resistivity of high-quality copper whiskers taking account of the surface scattering in different magnetic fields, the parameter  $A$  for the electrical resistivity of bulk copper has been estimated [38]. Temperature dependence of the scattering rate in copper has also been investigated by radio frequency size effect to determine the contribution of electron–electron collisions [39]. The observed  $T^4$  behavior for the low-temperature electrical resistivity of Ag is related to the simultaneous presence of both electron–phonon and electron–electron scattering [40]. To observe the term  $T^2$  in noble metals, very low temperatures and very pure metals are needed.

Aluminum is a simple polyvalent metal in which electron–electron scattering has been intensively investigated [41–44]. In [41], the electrical resistivity of aluminum at low temperatures is described by the term  $AT^2$ . The surface scattering contribution for electrical resistivity of high-purity aluminum samples in the thickness range from 0.1  $\mu\text{m}$  to 7 mm was investigated in [42]. It was shown that surface scattering of the conduction

electrons affects the temperature dependence of the resistivity for samples less than 0.5 mm in thickness. The electrical resistivity term  $AT^2$  is attributed to electron–electron scattering, and it has been shown that coefficient  $A$  practically does not depend on the residual resistivity value [43]. The influence of the electron–phonon interaction on electron–electron scattering is described within the framework of the Landau Fermi liquid theory, and electron–electron scattering contribution to the low-temperature resistivity of aluminum can be enhanced by a factor of  $\sim 20$  due to electron–phonon interaction [44].

Due to the fact that transition group metals differ from simple metals, which have partially filled  $d$ - and  $s$ -band electrons, it has been believed that for transition metals, the major contribution to resistivity  $\rho_{ee}(T)$  should be caused by highly mobile  $s$ -electrons being scattered by the “heavy”  $d$ -electrons, i.e., the so-called  $sd$ -scattering. It is observed that coefficient  $A$  for transition metals is often one or two orders of magnitude larger than for simple metals. Quadratic temperature dependence for  $\rho_{exp}(T)$  for many transition metals has been demonstrated at low temperatures [27,45–49], but interpretations are different. In [45], it is shown that there is some correlation between coefficient  $A_{exp}$  and the electronic heat capacity parameter  $\gamma$ . The electron–electron scattering in tungsten has been investigated by using radio-frequency size effect for electron scattering rate estimation [46]. The term  $AT^2$  has been found over the temperature range 1.5–5 K for molybdenum, and it was concluded that the quadratic term in the temperature dependence of the scattering rate in molybdenum is due to electron–electron scattering [47]. The electrical resistivity of a single crystal of vanadium at low temperatures has been analyzed in terms of electron impurity, electron–electron, and electron–phonon scatterings [48]. The term  $AT^2$  with coefficient  $A \approx (1.6–0.2) \cdot 10^{-11} \text{ } \Omega\text{cm}/\text{K}^2$  was obtained. The effects of electron–electron scattering in vanadium have been investigated theoretically, and the calculated scattering rates agree with experimental measurement results [27]. Electron–electron scattering in high-purity single crystals of molybdenum has been measured at low temperatures [49], and when approaching an ideal metallic crystal structure, there have been observed deviations from Ohm’s law.

The traditional explanation [10] for the large magnitude of  $A_{exp}$  due to  $sd$ -scattering in transition metals is based on the assumption that the effective mass of the  $d$ -electron is very high, implying that its velocity  $v_d$  is very low compared with the velocity  $v_s$  of the  $s$ -electron. These arguments are very questionable, because the drift mobility and drift velocity of metals (see Equations (2) and (3)) do not depend on the electron mass. All electrons at the Fermi surface have the same Fermi-level energy and are randomly moving with the same Fermi velocity.

We want to point attention to the fact that conservation of the quasi-momentum and energy of free electrons due to electron–electron scattering does not produce energy losses, and consequently, this process is elastic and has no effect on material resistivity. This is confirmed by the thermal noise relation with material resistivity [50] and by the fluctuation–dissipation theorem [51,52]. Therefore, for almost all elemental metals, electrical resistivity at low temperatures has the term  $AT^2$ , but its explanation by electron–electron scattering is doubtful.

In [13,14], it was shown that lattice atom vibrations produce not only the effective density of free randomly moving electrons  $n_{eff} = g(E_F)kT$  (here  $g(E_F)$  is the density of states at Fermi-level energy) but also the same density of electronic defects (not completely screened ions) is produced  $N_{eff} = n_{eff}$ . In Figure 2, the electronic defect dependence on temperature for aluminum and for the transition group metal tungsten are demonstrated. As can be seen, the effective density of the electronic defects even at a temperature of 1 K is higher than  $10^{18} \text{ cm}^{-3}$ , and these electronic defects cannot in principle be decreased, as can be achieved with residual defects.

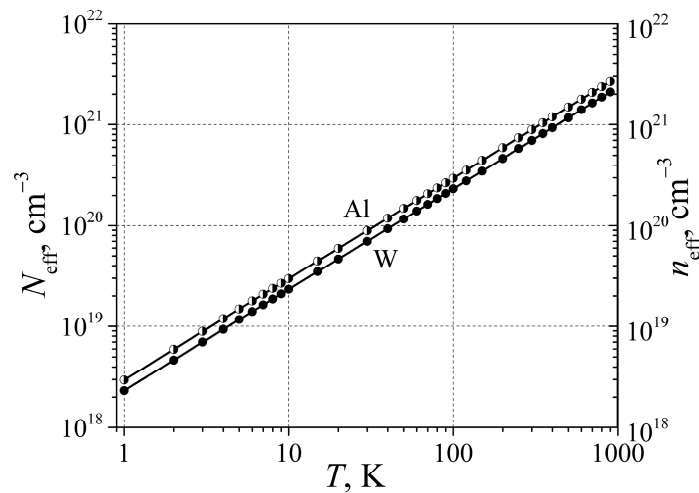


**Figure 2.** The electronic defect density  $N_{\text{eff}}$  (left scale), and free RM electron density  $n_{\text{eff}}$  (right scale) dependences on the temperature for metals Al and W.

As shown in [13,14], the resistivity of elemental metals' dependence on temperature can be described as:

$$\rho(T) = \rho_0 + \rho(T_0) \cdot (T/T_0) \cdot \eta_{\text{ph}}(T/\Theta) \tag{13}$$

where  $\Theta$  is the Debye temperature and  $\eta_{\text{ph}}(T/\Theta)$  is the phonon mediation factor accounting for the free RM electron scattering by electronic defects:

$$\eta_{\text{ph}}(T/\Theta) = (T/\Theta)^4 \int_0^{\Theta/T} \frac{4x^5 dx}{(e^x - 1)(1 - e^{-x})} \tag{14}$$

The resistivity  $\rho(T_0)$  at a temperature above room temperature  $T = T_0$  is described as:

$$\rho(T_0) = \frac{1}{q^2 g(E_F) D} = \frac{3}{q^2 g(E_F) l_F v_F} = \frac{3 \sigma_{\text{eff}0} k T_0}{q^2 v_F} \tag{15}$$

Here, we used  $l_F = 1/(\sigma_{\text{eff}0} N_{\text{eff}}) = 1/[\sigma_{\text{eff}0} g(E_F) k T_0]$ , where  $\sigma_{\text{eff}0}$  is the effective scattering cross section estimated at temperature  $T_0$ . The value of the temperature  $T_0$  must be taken from the linear resistivity range dependence on temperature. Then, the effective scattering cross section is estimated as:

$$\sigma_{\text{eff}}(T) = \sigma_{\text{eff}0} \eta_{\text{ph}}(T/\Theta) \tag{16}$$

For further study of the resistivity dependence on temperature, we shall investigate the elemental metals from various sites of the periodic tables: the alkali group metal Li, the noble metal Cu, the second group IIB metal Zn, the third group IIIA metal Al, and the transition group metals Mo and W. The resistivity dependences on temperature for these metals are presented in Figure 3: dots are the experimental results, and the solid lines are calculated by Equation (13). As can be seen, the resistivity  $\rho(T)$  of metals has three clearly expressed parts: (i) at low temperature, the so-named residual resistivity caused by impurity and structural imperfections of metal, (ii) the so-named phonon-assisted part with  $\rho \sim T^5$ , which at higher temperatures crosses to (iii) the linear resistivity dependence on temperature.

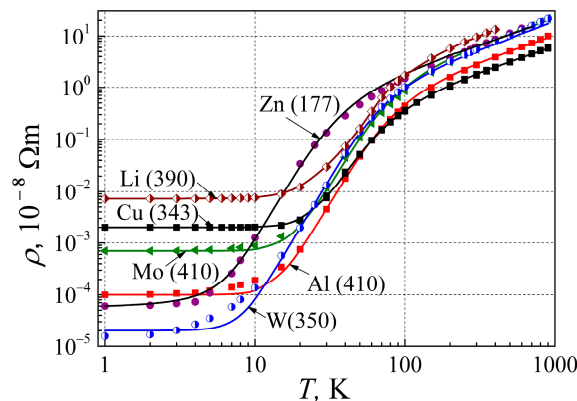


**Figure 3.** Resistivity dependence on temperature of elemental metals Al, Cu, Li, Mo, W, and Zn. Dots are experimental data from the *Handbook of Chemistry and Physics* [5], and solid lines are calculated by Equation (13). The number near the chemical symbol is Debye’s temperature of this metal used for calculations.

Even though the entire description of the resistivity of metals by Equation (13) is sufficiently good, at temperatures below 20 K, there is a small inadequacy for metals Al, Zn, Mo, and W. Considering the experimental results of the electrical resistivity term  $AT^2$  presented earlier, we shall see further what causes such electrical resistivity dependence on very low temperatures.

Considering the so-named law  $\rho = AT^2$  at low temperatures, we shall carefully investigate the resistivity dependence on low temperatures on a sample of Al. To this end, we shall find what characteristics cause such resistivity  $(\rho(T) - \rho_0)$  temperature dependence. In Figure 4 the resistivity  $\rho(T)$  and  $\rho(T) - \rho_0$  dependences on low temperatures for aluminum are presented.

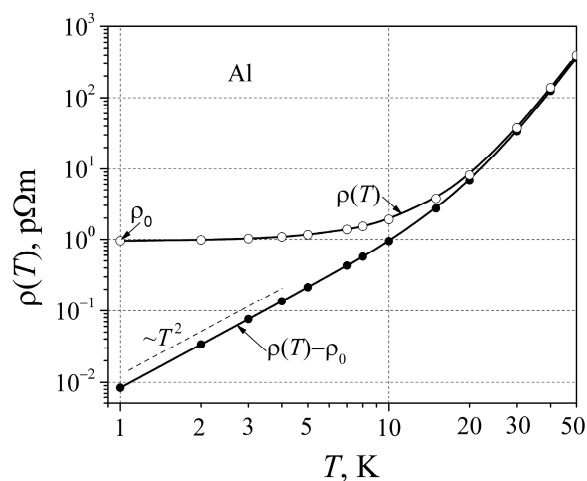


**Figure 4.** The aluminum electrical resistivity dependence on temperature at low temperatures.

As can be seen, the resistivity  $(\rho(T) - \rho_0)$  without residual resistivity  $\rho_0$  has a well-expressed dependence on temperature term  $AT^2$ , where the proportionality coefficient  $A \approx 6.5 \text{ f}\Omega\text{m K}^{-2}$ . Now the resistivity of metals can be described as  $\rho = (1/\sigma) = 1/[q^2g(E_F)D]$ , where  $D$  is the diffusion coefficient of free RM charge carriers. The diffusion coefficient of free RM charge carrier dependence on temperature is shown in Figure 5a. As can be seen, the diffusion coefficient at very low temperatures changes as  $T^{-2}$  and then crosses to the proportionality  $T^{-5}$  when the temperature is over 20 K.

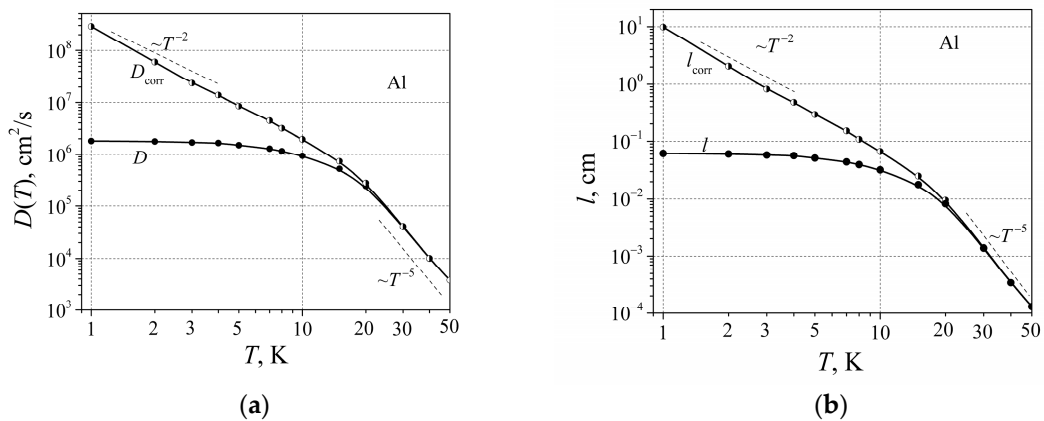


**Figure 5.** Diffusion coefficient (a) and mean free path (b) of free RM charge carrier dependence at low temperatures for Al.  $D = 1/[\rho(T)q^2g(E_F)]$ ,  $D_{\text{corr}} = 1/[(\rho(T) - \rho_0)q^2g(E_F)]$ , and  $l = 3D/v_F$ ,  $l_{\text{corr}} = 3D_{\text{corr}}/v_F$ .

The mean free path of charge carriers has been estimated as  $l = 3D/v_F$ , and  $l_{\text{corr}} = 3D_{\text{corr}}/v_F$ , and are presented in Figure 5b. As can be seen, the mean free path  $l_{\text{corr}}$  at very low temperatures changes as  $T^{-2}$ , and exceeds several centimeters. It seems that precise resistivity measurements should be conducted with a very large sample such that the transverse dimensions greatly exceed the mean path of the charge carriers in order to eliminate charge carrier scattering from the sample boundaries.

The relaxation time of charge carriers has been evaluated as  $\tau = l/v_F$  and  $\tau_{\text{corr}} = l_{\text{corr}}/v_F$ , and are presented in Figure 6a. It is believed that the relaxation time  $\tau_{\text{corr}}$  changes as  $T^{-2}$  at low temperatures. Now let us estimate the effective scattering cross section of free RM electrons by electronic defects.

$$\sigma_{\text{eff}} = \frac{1}{l_{\text{corr}}N_{\text{eff}}} = \frac{1}{l_{\text{corr}}g(E_F)kT} \tag{17}$$

where  $N_{\text{eff}}$  is the electronic defect density. The effective scattering cross section dependence on temperature is presented in Figure 6b. As can be seen, the effective scattering cross section at very low temperatures is proportional to temperature  $T$ , and at higher temperatures coincides with  $\sigma_{\text{eff}0}\eta_{\text{ph}}(T/\Theta)$  and is proportional to  $T^4$ . It seems that for the resistivity term  $AT^2$  at low temperatures, the solution key is related to the linear effective scattering cross-section dependence on temperature.

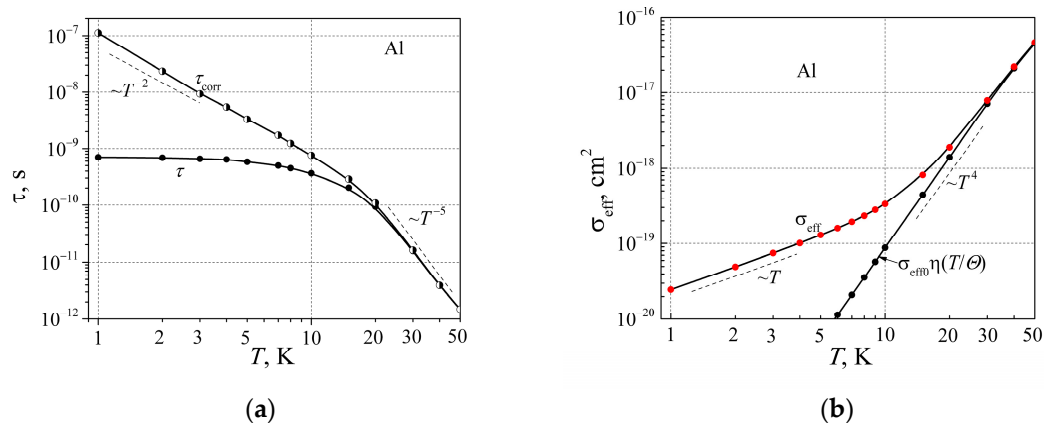


**Figure 6.** The relaxation time (a) and the effective scattering cross section (b) dependences on the temperature at low temperatures for aluminum (the  $\sigma_{\text{eff}}$  is described by Equation (17), and  $\sigma_{\text{eff}0}\eta_{\text{ph}}(T/\Theta)$  by Equation (16)).

In Figure 7, the heat capacity dependence on temperature for conductors (Pt and W), and pure Si, which at low temperatures is an insulator, is presented. The heat capacity of the insulator is described by Debye’s model, for which the heat capacity at low temperatures increases as  $T^3$  or the thermal energy (quantity of heat) increases as  $T^4$ . In the case of metals, the heat capacity at low temperatures changes more slowly, approximately linearly, and thermal energy changes as  $T^2$ . As can be seen, the metal of the one-mole mass at temperature 5 K has greater heat than the insulator. This difference is related to the free electron excitation and their random movement, and due to their scattering by electronic defects. In equilibrium, the thermal energies between free electrons and lattice atoms are changing by the interaction of free electrons with the electronic defects.

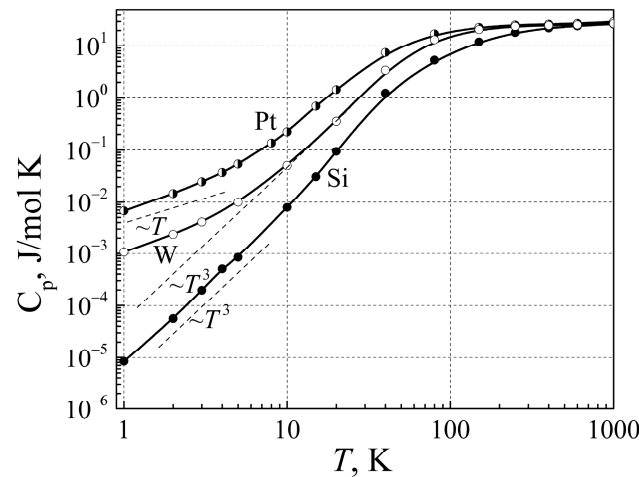


**Figure 7.** Experimental data of the heat capacity dependence on temperature for conductors (Pt and W) and silicon. Experimental data are taken from the Handbook of Physical Quantities [6].

Earlier, for estimation of the phonon mediation factor  $\eta_{ph}(T/\Theta)$ , Equation (14) accounted only for the lattice thermal energy based on the Debye model. Additional thermal energy for conductors is caused by free randomly moving charge carriers, which are scattered by electronic defects. This necessitates a correction of the phonon mediation factor  $\eta_{ph}(T/\Theta)$ :

$$\eta(T) = (T/\Theta)^4 \int_0^{\Theta/T} \frac{4x^5 dx}{(e^x - 1)(1 - e^{-x})} + \Delta\eta_{ph}(T) \tag{18}$$

where the correction factor:

$$\Delta\eta_{ph}(T) = \frac{\Delta E_{ph1}}{E_{e1}} \tag{19}$$

is equal to the ratio between the ratio of the thermal (phonon) energy increase  $\Delta E_{ph1}$  of the metal atom caused by free RM electron interaction with electronic defects and the average free RM electron energy  $E_{e1} = 1.64 kT$  at low temperatures. The variation in the thermal energy of the metal atom due to interaction with free randomly moving electrons can be estimated as:

$$\Delta E_{ph1} = \left[ \left( \frac{\pi^2}{6} \right) g(E_F) (kT)^2 / N_A \right] \tag{20}$$

where  $N_A$  is the Avogadro constant. Equation (20) can be rewritten as:

$$\Delta E_{ph1} = (1/2) \gamma T^2 / N_A \tag{21}$$

where  $\gamma$  is the electronic heat capacity parameter. Then, the correction factor can be described in the following form:

$$\Delta\eta_{ph}(T) = \frac{\gamma T^2}{2E_{e1}N_A} = \frac{\gamma T^2}{3.28kTN_A} = \frac{\gamma T}{3.28R} \tag{22}$$

where  $R = kN_A = 8.31 \text{ J}/(\text{mol K})$  is the universal gas constant.

Therefore, the corrected phonon mediation factor can be presented as:

$$\eta(T) = \frac{\gamma T}{3.28R} + (T/\Theta)^4 \int_0^{\Theta/T} \frac{4x^5 dx}{(e^x - 1)(1 - e^{-x})} \tag{23}$$

and the resistivity can be described as:

$$\rho(T) = \rho_0 + \rho(T_0) \cdot (T/T_0) \cdot \eta(T) \tag{24}$$

and:

$$\rho(T) - \rho_0 = \rho(T_0) \cdot (T/T_0) \cdot \eta(T) \tag{25}$$

Now let us describe the elemental metals from different columns of the periodic table: Al, W, Mo, Zn, Li, and Cu resistivity dependences in a very wide temperature range accounting for the obtained correction factor. In Figure 8a, resistivity and corrected phonon mediation factor dependences on temperature for aluminum are presented, and those for tungsten in Figure 8b. In Figure 8, the small black dots are the experimental dots of the resistivity [5] and the solid black line calculated by Equation (24). The red dots are experimental data of  $(\rho(T) - \rho_0)$ , the solid red line is calculated by Equation (25), the corrected phonon mediation factor  $\eta(T)$  is calculated by Equation (23), and the dashed line proportional to  $T^{-4}$  is estimated by Equation (14) for the phonon mediation factor without correction. From the comparison of the resistivity  $(\rho(T))$  curves in Figures 2 and 8a, it is seen that Equation (24) describes the experimental results below 25 K temperature very well. As can be seen from Figure 8a, at low temperatures, the resistivity  $(\rho(T) - \rho_0) \approx AT^2$ , where  $A \approx 6 \text{ f}\Omega\text{m}/\text{K}^2$ .

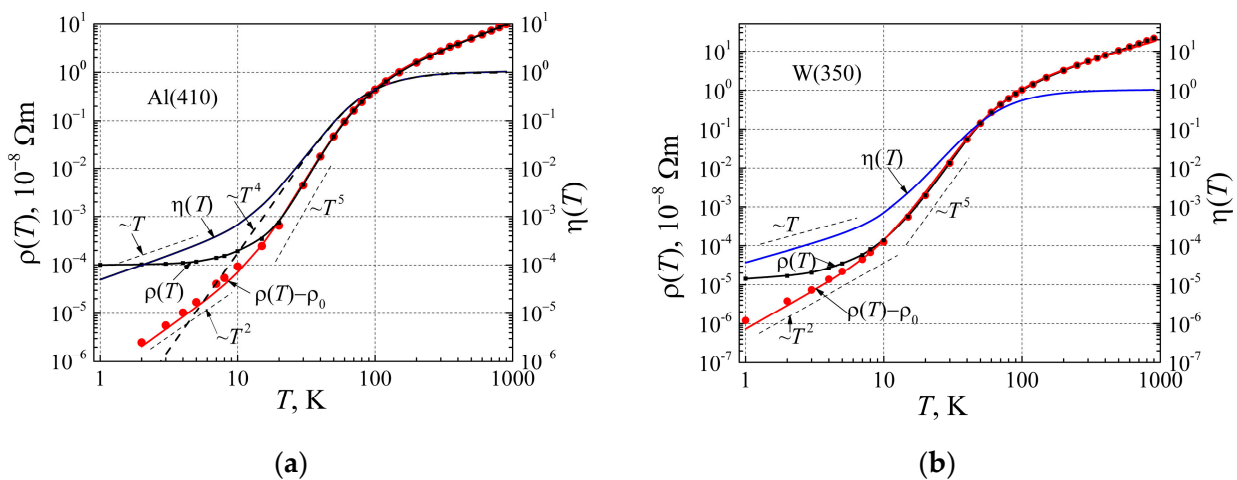


**Figure 8.** Resistivity (left scale) and corrected phonon mediation factor  $\eta(T)$  (right scale) dependences on temperature for aluminum (a) and tungsten (b).

The similar results in Figure 8b to aluminum (Figure 8a) are the investigation results for tungsten. Though tungsten has double the valence electrons of aluminum, the DOS  $g(E_F)$  of tungsten is about 1.3 times smaller than that of aluminum. The residual resistivity of a given sample of tungsten is about 10 times smaller than that of aluminum. The difference between resistance  $\rho(T)$  and  $(\rho(T) - \rho_0)$  at low temperatures for aluminum begins at  $T < 20 \text{ K}$ , while for tungsten it is at  $T < 8 \text{ K}$  and the coefficient  $A \approx 8 \text{ f}\Omega\text{m}/\text{K}^2$ . The phonon mediation factor  $\eta(T)$  dependences on temperature are almost the same for both metals.

In Figure 9a, resistivity and corrected phonon mediation factor dependences on temperature for molybdenum are presented, and those for zinc in Figure 9b. Debye's temperature obtained from resistivity dependence on temperature for Mo and Al is the same, 410 K, and corrected phonon mediation factors are close to one another, while the residual resistivity of a given sample of molybdenum is about 10 times larger than that of aluminum. The resistivity  $(\rho(T) - \rho_0)$  proportionality to  $T^2$  for molybdenum is obtained at  $T < 10$  K. The characteristics of the two-valent zinc (Figure 9b) differ from those of molybdenum (Figure 9a). This is related to Debye's temperature of zinc (177 K), which is less than half that of Mo (410 K), representing a shift in resistivity characteristics at lower temperatures. In addition, the DOS  $g(E_F)$  of zinc is about half that of molybdenum. As a consequence, the linear part of the phonon mediation factor begins at a lower temperature, which causes resistivity  $(\rho(T) - \rho_0)$  proportionality to  $T^2$ , which would be observed only at  $T < 4$  K.

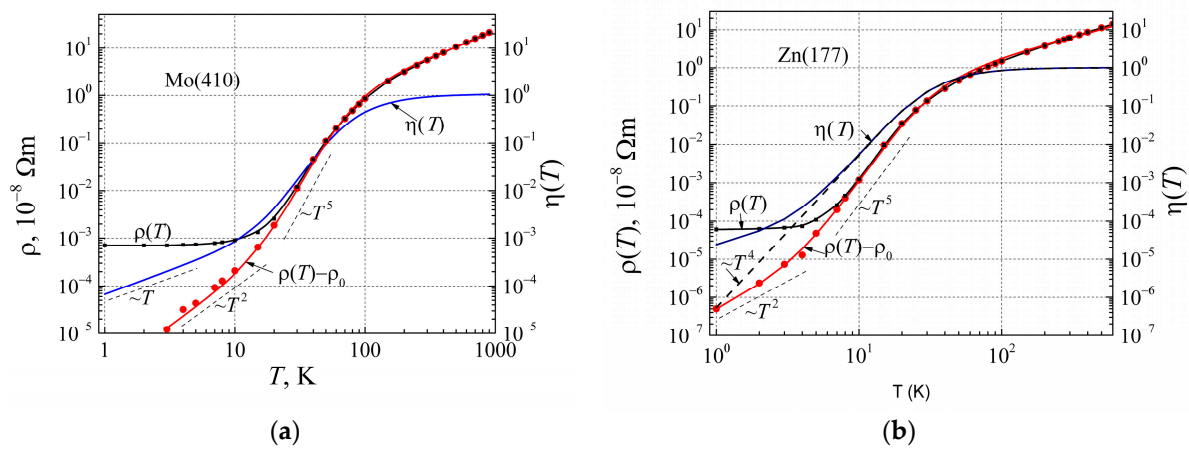


**Figure 9.** Resistivity (left scale), and corrected phonon mediation factor (right scale) dependences on temperature for molybdenum (a) and zinc (b).

In Figure 10, the resistivity and corrected phonon mediation factor dependences on temperature for copper and lithium are presented. Considering that the presented sample of the copper resistivity data has sufficiently high residual resistivity, it was not possible to observe the  $T^2$  dependence on temperature (Figure 10a). As seen in this figure, the resistivity  $(\rho(T) - \rho_0)$  changes at low temperatures approximate to  $T^4$ , and similar behavior has been observed for other noble metals [37,40]. On the other hand, the linear part of the corrected phonon mediation factor begins only below 4 K, and from this, it follows that the resistivity law  $AT^2$  can be obtained at resistivity values smaller than 10 f $\Omega m$ . This perhaps explains why the resistivity law  $AT^2$  for noble metals is difficult to obtain. In Figure 10b, the resistivity and corrected phonon mediation factor dependences for lithium are presented. As can be seen, the linear part of the corrected phonon mediation factor begins below 7 K, the square resistivity dependence on temperature is observed at a temperature below 7 K, and the proportionality coefficient  $A$  is approximately equal to 20 f $\Omega m/K^2$ .

As can be seen, the resistivity  $(\rho(T) - \rho_0)$  proportionality to  $T^2$  at low temperatures is observed for alkali, noble, simple polyvalent, or transition group metals, and temperatures at which it takes place depend on both the Debye temperature and the DOS at the Fermi surface of metals.

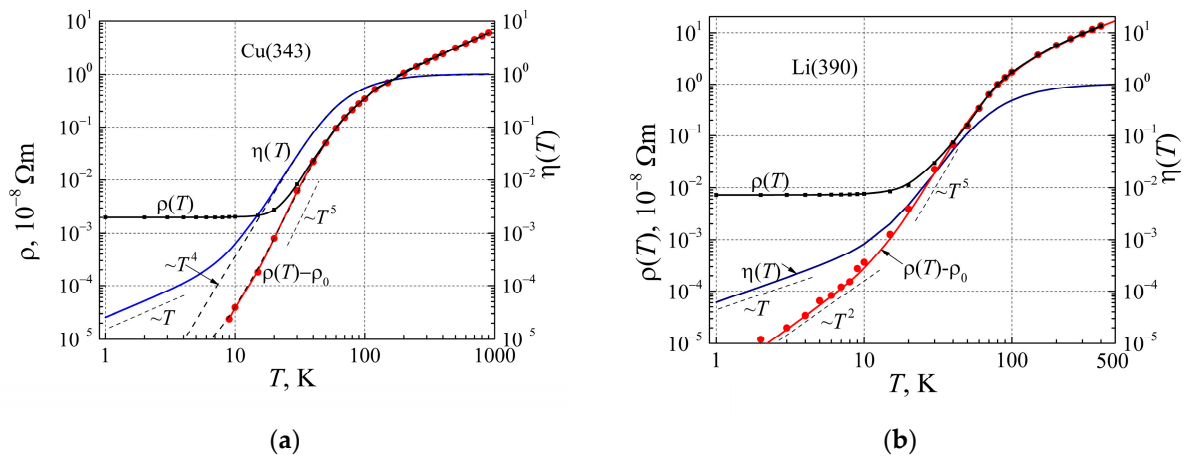


**Figure 10.** The resistivity (left scale) and corrected phonon mediation factor (right scale) dependences on temperature for copper (a) and lithium (b).

In Figure 11, the effective electron scattering cross-section dependences on temperature for the analyzed metals Al, Cu, Li, Mo, W, and Zn are presented. As can be seen, the effective free electron scattering cross-section dependences on temperature have three characteristic parts: (i) the linear  $\sim T$  at  $T < 10$  K; (ii) proportionality to  $T^4$  in the transition temperature range below Debye's temperature; and (iii) the constant at  $T > 200$  K. The constant part of the effective free electron scattering cross section shows that earlier explanations that the free electron scattering cross section at room and higher temperatures increases proportionally to temperature  $T$  due to lattice atom vibrations [7–11,19–22] are unfounded. The linear  $\eta(T)$  increase at very low temperatures is caused by the linear heat capacity increase with temperature, which causes the quadratic resistivity of elemental metal dependence on temperature. Therefore, this demonstrates that the earlier explanation of metal resistivity by electron–electron scattering at very low temperatures is not acceptable.

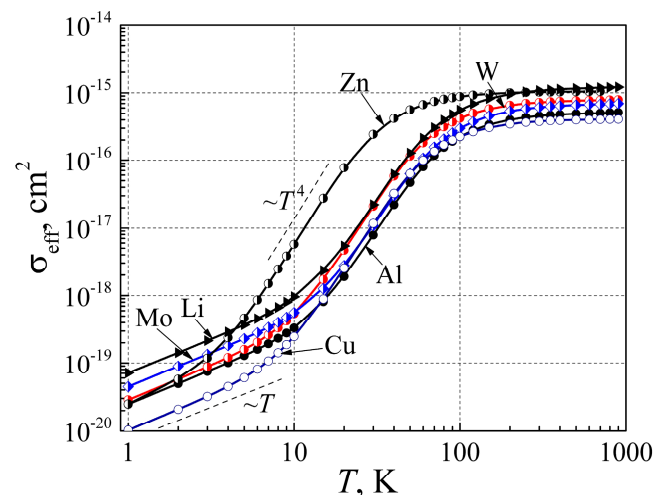


**Figure 11.** Effective free RM electron scattering cross-section dependences on temperature for metals Al, Cu, Li, Mo, W, and Zn.

From free RM electron effective scattering cross-section dependence on temperature follows such resistivity of elemental metal dependence on temperature characteristics: (i) the quadratic term  $AT^2$  at  $T < 10$  K (by eliminating the residual resistivity), (ii) the term  $\sim T^5$  in the transition temperature range below Debye's temperature, and (iii) the linear term  $\sim T$  at  $T > 200$  K. The whole resistivity (including the residual resistivity) temperature dependence is described by Equation (24) and accounts for the corrected phonon mediation

factor (Equation (23)), i.e., the elemental metal resistivity in the overall temperature range can be explained by free random electron scattering by electronic defects, accounting for the phonon mediation factor.

#### 4. Conclusions

Given that the Einsteinian relation between the diffusion coefficient and the drift mobility of free randomly moving electrons in a metal is always valid, the effective electric force in metals is enhanced by a factor of  $\alpha_\epsilon = E_F/kT$ . Free RM electrons are scattered only by electronic defects (weakly screened ions, which lose the valence electrons), the electron wave vector during a collision with an electronic defect changes very remarkably, and after each collision, the electron wave vector direction is completely random. The electrical resistivity of almost all elemental metals at very low temperatures has the term  $AT^2$ , which has been explained on the base of the Landau and Pomeranchuk Fermi liquid model by electron–electron scattering. In this work, it is shown that the electrical resistivity term  $AT^2$  at very low temperatures is caused by free RM electron scattering by electronic defects, i.e., it is related to the linear effective scattering cross-section dependence on temperature due to free RM electron scattering by electronic defects. The value of the parameter  $A$  depends on both the DOS at the Fermi surface and the Debye temperature. It is shown that the effective scattering cross section of the free RM electrons by electronic defect dependence on temperature has three characteristic parts: (i) constant at  $T > 200$  K, (ii) proportionality to  $T^4$  in the transition range below the Debye temperature, and (iii) linear  $\sim T$  at very low temperatures.

**Funding:** The research received no external funding.

**Data Availability Statement:** The raw data supporting the conclusions of this article will be made available by the authors on request.

**Conflicts of Interest:** The author declares no conflicts of interest.

#### References

1. Drude, P. Zur Elektronentheorie der Metalle. *Ann. Phys.* **1900**, *306*, 441–624. [\[CrossRef\]](#)
2. Kaxiras, E. *Atomic and Electronic Structure of Solids*; Cambridge University Press: Cambridge, UK, 2014.
3. Sander, L.M. *Advanced Condensed Matter Physics*; Cambridge University Press: Cambridge, UK, 2014.
4. Blakemore, J.S. *Solid State Physics*; Cambridge University Press: Cambridge, UK, 1985.
5. Lide, D.E. (Ed.) *Handbook of Chemistry and Physics*, 84th ed.; CRC Press LLC: Boca Raton, FL, USA, 2004.
6. Grigoryev, L.S.; Meilikhov, E.Z. (Eds.) *Handbook of the Physical Quantities*; Energoatomizdat: Moscow, Russia, 1991.
7. Mizutani, U. *Introduction to the Electron Theory of Metals*; Cambridge University Press: Cambridge, UK, 2014.
8. Dugdale, J.S. *The Electrical Properties of Disordered Metals*; Cambridge University Press: Cambridge, UK, 1985.
9. Ashcroft, N.W.; Mermin, N.D. *Solid State Physics*; Harcourt College Publ.: New York, NY, USA, 1976.
10. Ziman, J.M. *The Theory of Transport Phenomena in Solids*; Oxford University Press: Oxford, UK, 2001.
11. Kittel, C. *Introduction to Solid State Physics*; John Wiley and Sons, Inc.: New York, NY, USA, 1976.
12. Blokhintsev, D.L. *Quantum Mechanics*; Reidel Publ. Comp.: Dordrecht, The Netherlands, 1964.
13. Palenskis, V.; Žitkevičius, E. Summary of new insight into electron transport in metals. *Crystals* **2021**, *11*, 622. [\[CrossRef\]](#)
14. Palenskis, V.; Jonkus, V. Study of the free randomly moving electron transport peculiarities in metals. *Metals* **2023**, *13*, 1551. [\[CrossRef\]](#)
15. Palenskis, V. Drift mobility, diffusion coefficient of randomly moving charge carriers in metals and other materials with degenerate electron gas. *World J. Cond. Matt. Phys.* **2013**, *3*, 73–81. [\[CrossRef\]](#)
16. Palenskis, V. The effective density of randomly moving electrons and related characteristics of materials with degenerate electron gas. *AIP Adv.* **2014**, *4*, 047119.
17. Stirzaker, D.R. *Elementary Probability*; Cambridge University Press: Cambridge, UK, 2014.
18. Grimmet, G.R.; Stirzaker, D.R. *Probability and Random Processes*; Cambridge University Press: Cambridge, UK, 2020.
19. Abrikosov, A.A. *Fundamentals of the Theory of Metals*; North-Holland Publication: Amsterdam, The Netherlands, 1988.
20. Lundstrom, M. *Fundamentals of Carrier Transport*; Cambridge University Press: Cambridge, UK, 2014.
21. Rossiter, P.L. *The Electrical Resistivity of Metals and Alloys*; Cambridge University Press: Cambridge, UK, 2014.
22. Schulze, G.E.R. *Metallphysik*; Akademie-Verlage: Berlin, Germany, 1967.
23. Landau, L.D.; Pomeranchuk, I.Y. On properties at very low energies. *Zh. Eksp. Teor. Phys.* **1937**, *7*, 379.
24. Kaveh, M.; Wiser, N. Electron-electron scattering in conducting materials. *Adv. Phys.* **1984**, *33*, 257–372. [\[CrossRef\]](#)

25. Schulz, W.W.; Allen, P.A. Transport in metals with electron-electron scattering. *Phys. Rev. B* **1995**, *52*, 7994. [[CrossRef](#)]
26. Arulsamy, A.D. Low-temperature small-angle electron-electron scattering rate in Fermi metals. *Z. Nat. A* **2024**, *79*, 83–99. [[CrossRef](#)]
27. Potter, C.; Morgan, G.J. Electron-electron scattering effects in metals. *J. Phys. F Met. Phys.* **1979**, *9*, 493. [[CrossRef](#)]
28. Van Kampen, H.; Neyenhuisen, H.W.; Ribot, J.H.J.M. Semiautomatic bridge for high-precision dc resistance measurements on pure metals at low temperatures. *Rev. Sci. Instrum.* **1979**, *50*, 161–164. [[CrossRef](#)] [[PubMed](#)]
29. Zwart, J.W.; Pratt, W.P.; Schroeder, P.A.; Caplic, A.D. High-precision measurements of the resistivity of strained dilute copper-silver alloys below 1 K. *J. Phys. Met. Phys.* **1983**, *13*, 2595–2602. [[CrossRef](#)]
30. Barnard, B.R.; Caplin, A.D. A simple high-resolution cryogenic resistance bridge using a SQUID null detector. *J. Phys. E Sci. Instrum.* **1978**, *11*, 1117. [[CrossRef](#)]
31. Kaveh, M.; Wisser, N. General theory of the electrical resistivity of the alkali metals at low temperatures. *Phys. Rev. B* **1974**, *9*, 4042. [[CrossRef](#)]
32. MacDonald, A.H.; Taylor, R.; Geldart, D.J.W. Umklapp electron-electron scattering and the low-temperature electrical resistivity of the alkali metals. *Phys. Rev. B* **1981**, *23*, 2718. [[CrossRef](#)]
33. Kaveh, M.; Wisser, N. Electrical resistivity of potassium at low temperatures. *Phys. Rev. B* **1974**, *9*, 4053.
34. Van Kampen, H.; Ribot, J.H.J.M.; Wyder, P. The electrical resistivity of potassium at low temperatures. *J. Phys. Met. Phys.* **2000**, *11*, 597.
35. Awasthi, O.N.; Pundhir, V.K. Electron-electron interactions and the electrical resistivity of lithium at low temperatures. *Pramana J. Phys.* **2007**, *68*, 67–74.
36. Sinvani, M.; Greenfield, A.; Danino, M.; Kaveh, M.; Wisser, N. Anomalous electron-electron scattering contribution to the electrical resistivity of lithium. *J. Phys. F Met. Phys.* **1981**, *11*, L73. [[CrossRef](#)]
37. Sathish, S.; Awasthi, O.N. Electron-electron scattering and low-temperature electrical resistivity in copper and silver. *Phys. Lett. A* **1984**, *100*, 215–217. [[CrossRef](#)]
38. Thummes, G.; Kötzler, J. Magnetic-field-enhanced electron-electron scattering in the resistivity of copper. *Phys. Rev. B* **1985**, *31*, 2535. [[CrossRef](#)] [[PubMed](#)]
39. Gasparov, V.A.; Harutunian, M.H. To the question on electron-electron scattering in metals. *Solid State Commun.* **1976**, *19*, 189–192. [[CrossRef](#)]
40. Bergmann, A.; Kaveh, M.; Wisser, N. Explanation of the anomalous  $T^4$  behaviour of the low-temperature electrical resistivity of silver. *J. Phys. F Met. Phys.* **1980**, *10*, L71. [[CrossRef](#)]
41. Kaveh, M.; Wisser, N. Evidence for the electron-electron scattering contribution to the electrical resistivity of aluminum. *Phys. Lett. A* **1975**, *51*, 89–90. [[CrossRef](#)]
42. Sambles, J.R.; Elsom, K.C.; Sharp-Dent, G. The effect of sample thickness on the resistivity of aluminum. *J. Phys. F Met. Phys.* **1981**, *11*, 1075. [[CrossRef](#)]
43. Ribot, J.H.J.M.; Bass, J.; Van Kampen, H.; Wyder, P. Further evidence for electron-electron scattering in aluminum. *J. Phys. F Met. Phys.* **1981**, *9*, L117. [[CrossRef](#)]
44. MacDonald, A.H. Electron-phonon enhancement of electron-electron scattering in Al. *Phys. Rev. Lett.* **1980**, *44*, 489. [[CrossRef](#)]
45. Volkenshtein, N.V.; Novoloselov, V.A.; Startsev, V.E. Role of interelectron collisions in the electric resistance of transition metals. *Sov. Phys. JETP* **1971**, *33*, 58–587.
46. Van der Mass, J.; Huguenin, R.; Gasparov, V.A. Electron-electron scattering in tungsten. *J. Phys. F Met. Phys.* **1985**, *15*, L271. [[CrossRef](#)]
47. Gasparov, V.A.; Voloshin, I.F.; Fisher, L.M. On electron-electron scattering in molybdenum. *Solid State. Commun.* **1979**, *29*, 43–46. [[CrossRef](#)]
48. Gautron, G.J.; Zablocki, J.E.; Hsiang, T.Y.; Weinstock, H.; Schmidt, F.A. Electron-electron scattering in vanadium. *J. Low Temp. Phys.* **1982**, *49*, 185–191. [[CrossRef](#)]
49. Elefant, D. Limits of Ohm's law in ultra-pure metals with almost ideal crystal lattices. *J. Appl. Phys.* **2023**, *134*, 205102. [[CrossRef](#)]
50. Nyquist, H. Thermal agitation of electric charge in conductors. *Phys. Rev.* **1928**, *32*, 110–113. [[CrossRef](#)]
51. Kubo, R. Statistical-mechanical theory of irreversible processes. I. General theory and simple applications to magnetic and conduction problems. *J. Phys. Soc. Jap.* **1957**, *12*, 570–586. [[CrossRef](#)]
52. Kubo, R.A. General expression for the conductivity tensor. *J. Phys.* **1956**, *34*, 1274–1277. [[CrossRef](#)]

**Disclaimer/Publisher's Note:** The statements, opinions and data contained in all publications are solely those of the individual author(s) and contributor(s) and not of MDPI and/or the editor(s). MDPI and/or the editor(s) disclaim responsibility for any injury to people or property resulting from any ideas, methods, instructions or products referred to in the content.